

A Spatially Detailed Approach to the Assessment of Rooftop Solar Energy Potential based on LiDAR Data

Mohammad Aslani¹ and Stefan Seipel^{1,2}

¹*Department of Computer and Geo-spatial Sciences, University of Gävle, Gävle, Sweden*

²*Division of Visual Information and Interaction, Department of Information Technology, Uppsala University, Uppsala, Sweden*

Keywords: Deep Learning, Clustering, Segmentation, Solar Energy, LiDAR.

Abstract: Rooftop solar energy has long been regarded as a promising solution to cities' growing energy demand and environmental problems. A reliable estimate of rooftop solar energy facilitates the deployment of photovoltaics and helps formulate renewable-related policies. This reliable estimate underpins the necessity of accurately pinpointing the areas utilizable for mounting photovoltaics. The size, shape, and superstructures of rooftops as well as shadow effects are the important factors that have a considerable impact on utilizable areas. In this study, the utilizable areas and solar energy potential of rooftops are estimated by considering the mentioned factors using a three-step methodology. The first step involves training PointNet++, a deep network for object detection in point clouds, to recognize rooftops in LiDAR data. Second, planar segments of rooftops are extracted using clustering. Finally, areas that receive sufficient solar irradiation, have an appropriate size, and fulfill photovoltaic installation requirements are identified using morphological operations and predefined thresholds. The obtained results show high accuracy for rooftop extraction (93%) and plane segmentation (99%). Moreover, the spatially detailed analysis indicates that 17% of rooftop areas are usable for photovoltaics.

1 INTRODUCTION

Solar energy generated by rooftop photovoltaics is a practical renewable energy resource that may provide a portion of the energy demand of buildings in urban areas (Joshi et al., 2021). Rooftop photovoltaics convert each building from a passive power consumer to an active power provider with low investment, thanks to the steep decline in their deployment costs (Bódis et al., 2019).

However, not all rooftop areas are utilizable for photovoltaic deployment. Utilizable rooftop areas are limited by various factors, the most important of which are the shape, orientation, and superstructures of roofs, as well as occlusion (Thebault et al., 2020). A rooftop with proper orientation and no superstructures or surrounding objects offers high solar energy potential. In contrast, a north-facing rooftop with many superstructures surrounded by tall buildings (in the northern hemisphere) may not offer high solar energy potential. In addition, the rooftop's geographical location and the local climate conditions may affect its solar energy potential.

Manually finding utilizable rooftop areas by considering the mentioned factors is laborious and impractical, particularly in large areas. Analyzing LiDAR datasets has been recognized as a potential way to automate this laborious process (Gassar and Cha, 2021). LiDAR datasets provide the 3D spatial profiles of the area and allow for automatic computation of characteristics of rooftops and their surrounding objects, such as area, height, tilt, and azimuth. In this context, one of the common methods of estimating the total utilizable areas is by applying a set of coefficients that consider roof types (e.g., flat or tilted), obtained from LiDAR datasets (Byrne et al., 2015). However, adjusting coefficients in heterogeneous regions is nontrivial, and thus the methods may lead to inaccurate results. To address this issue, spatially-based methods using geographical information systems (GIS) have been proposed, in which roof shapes are first modeled, and then their utilizable areas are identified by considering the tilts and orientations of roofs.

To model the shapes of roofs, it is necessary to first extract the footprints of rooftops. Numerous tech-

niques have been suggested for rooftop extraction. In this context, machine learning-based methods have shown high potential. In (Aslani and Seipel, 2020), support vector machines (SVMs) were employed to identify rooftops. A new method named data reduction based on locality sensitive hashing (DRLSH) was proposed to automatically select instances for training SVMs. In (Aslani and Seipel, 2021), another instance selection method for SVMs was developed, and it was tested on a dataset for rooftop extraction. In (Shin et al., 2022), PointNet++, a deep network, was used to identify rooftops from LiDAR datasets.

Once rooftops have been extracted, their shape (form) can be modeled. In (Lingfors et al., 2017), roofs were modeled using a predefined library of roof shapes for the purpose of estimating solar energy potential. More specifically, a model library that contains common roof shapes (e.g., gable and shed) was first defined, and the shape that best matches the corresponding point clouds was chosen. Following this method, in (Mohajeri et al., 2018), SVMs were used to choose the best-fitting roof shape from a predefined library. However, this type of roof shape modeling may overlook roof superstructures (e.g., chimneys), which play an important role in identifying utilizable areas. In (Sampath and Shan, 2010), another type of approach was used in which roofs are modeled by aggregating their constituent planar patches (roof faces) extracted by plane segmentation. They used fuzzy k-means clustering for plane segmentation. To enhance clustering, a planarity test that distinguishes planar from non-planar points was incorporated. In (Chen et al., 2014), a RANSAC-like algorithm was used for plane segmentation. In (Huang et al., 2015), region growing was utilized for segmenting planar patches. Unsuitable roof faces were then removed by applying area, slope, aspect, and solar irradiation thresholds. This approach does not require a predefined library of roof shapes and can model any polyhedral roof shape.

Most of the current spatially-based methods for identifying utilizable areas are limited to manual digitization or simplified roof shape modeling, and they may not consider shadow effects. This research identifies utilizable areas with more spatial details by considering roof shapes, roof superstructures, and shadow effects. Our methodology uses LiDAR data to assess the solar energy potential of rooftops in any area. It aims to automatically (a) extract rooftops using a deep learning-based method, (b) segment planar rooftop patches using a clustering-based method, and (c) identify utilizable areas using morphological operations.

2 METHODOLOGY

This section describes our methodology for automatically assessing rooftop solar energy potential. It leverages LiDAR datasets and assumes that they have sufficient density to model the shape and desired superstructures of roofs. LiDAR data contain 2.5D information about an area that can be used to model rooftops and solar irradiation. The methodology consists of three main steps (Figure 1), explained in further detail in the following subsections.

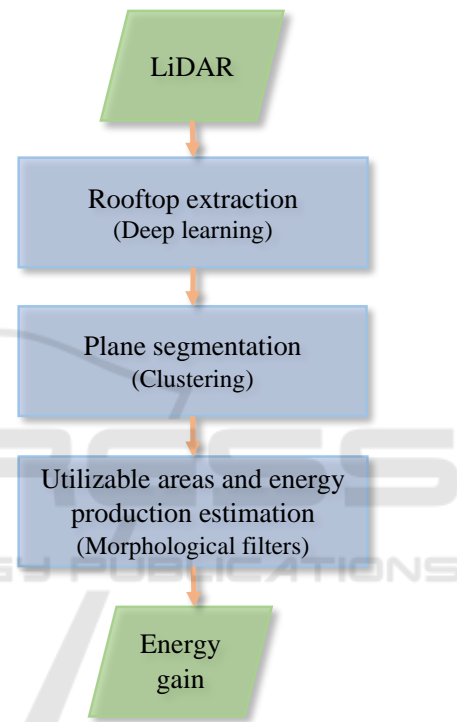


Figure 1: Overview of the methodology.

2.1 Rooftop Extraction

Extracting rooftops is required to determine the suitable areas where photovoltaics may be mounted. Rooftop extraction is a semantic segmentation task in which the points that comprise rooftops are identified. Owing to the remarkable advancements of deep learning methods and their satisfactory performance in doing semantic segmentation tasks, they are used in this step. In particular, we use PointNet++ to segment rooftops in LiDAR data (Qi et al., 2017). PointNet++ is a hierarchical neural network for semantic segmentation of unorganized point data, and it enables multi-scale point feature learning. It has the potential to be trained without requiring parameters that are specific to objects in LiDAR. A PointNet++ network con-

sists of three layers: sampling, grouping, and mini-PointNet layers. The sampling layer chooses a set of points that forms the centroids of local regions. The grouping layer constructs local regions sets around the centroids. The mini-PointNet layer abstracts the sets of local features into higher-level representations using a series of convolution, normalization, relu, and max-pooling layers. Please refer to (Qi et al., 2017) for more details. To train PointNet++ for rooftop extraction, we use labeled point clouds containing those features (please see Section 3).

2.2 Plane Segmentation

In this step, the constituent planar patches of rooftops are segmented. This step is required as photovoltaics are installed by considering planar segments of roofs. A digital surface model (DSM) is created from the recognized rooftop points using interpolation. This conversion makes the plane segmentation procedure easier.

Plane segmentation is performed based on clustering the normal vectors of pixels. A normal vector of a pixel is perpendicular to the surface at the pixel, and it is computed by fitting a plane to the pixel and its neighbors. Pixels on the same planar patch have similar normal vectors, and thus, by grouping them together, planar patches can be identified. Some pixels in each planar segment may, however, have normal vectors that are inconsistent with those of other pixels in the same segment. These pixels are known as non-planar pixels as they are placed in the vicinity of more than one plane. Including these pixels in clustering may disturb the creation of planar segments since they shatter the boundaries of clusters of normal vectors. As a result, non-planar pixels must be identified and excluded from clustering. The planarity of each pixel is evaluated based on the Eigenvalues of a 3D covariance matrix of the pixel and its neighbors (Awrangjeb and Fraser, 2014).

Initial planar segments are created by clustering the normal vectors of planar pixels. To delineate clusters, a minimum density divisive clustering (MDDC) algorithm was used (Tasoulis et al., 2016). Its adaptability (i.e., it requires no input parameters) and high computational efficiency make it suitable for handling large-scale plane segmentation. Since segmentation using MDDC does not consider the spatial connectivity of pixels, each resulting patch may comprise multiple parallel planar segments that are spatially separated. To split multi-part patches, Euclidean clustering based on pixel coordinates is applied (Rusu, 2009). Finally, the non-planar pixels, initially excluded, are assigned to the best segment using re-

gion growing. In this way, the problem of over-segmentation that may arise in clustering is also resolved. This plane segmentation method can identify all planar segments of a rooftop, even superstructures, to the extent that the spatial resolution of the DSM allows.

2.3 Utilizable Areas and Energy Production Estimation

This step involves computing the solar energy potential of rooftops. As photovoltaics cannot be installed over the entire area of a rooftop, it is necessary to ascertain areas utilizable for photovoltaics to avoid overestimation of energy production. Utilizable areas are defined as parts of rooftops where photovoltaics can be reasonably installed. In this research, each planar segment is spatially scrutinized to identify its utilizable areas.

Parts of planar segments should be kept free of photovoltaics to ease accessibility as an installation requirement of panels. Often, there should be a distance between the edge of photovoltaics and the segment that is known as service areas. To exclude these areas, we utilize a morphological erosion operation with a circular structuring element whose radius is equal to the width of the service areas (Sundararajan, 2017). The erosion operation shrinks the roof face by the width of the service area. In addition to service areas, there might be some areas of planar segments that are too small for a photovoltaic to fit, and these areas should be excluded. To do so, the algorithm suggested in (Aslani and Seipel, 2022) is employed in this paper. It iteratively applies a series of morphological opening operations and then aggregates their results. The structuring elements of the opening operations represent a photovoltaic with different rotations. The length and width of the structural elements are the same length and width as the photovoltaics that are being used.

After removing geometrically unsuitable areas, the remaining planar segments are evaluated in terms of solar irradiation. The segments whose average solar irradiation is below a specific threshold SI are removed. This is because photovoltaics are usually not installed on rooftop areas with low solar irradiation. In this way, planar segments that are mainly in shadow or those with unsuitable tilts (e.g., too steep) or azimuths (e.g., north-facing) are discarded. It should be noted that the solar irradiation of each segment is estimated using the solar model of ArcGIS Desktop (Fu and Rich, 2000; Rich et al., 1994). The solar model incorporates viewshed analysis to account for shadowing effects. The viewshed analy-

sis generates a Boolean image indicating the extent to which the sky is obscured by surrounding objects as seen from a certain place in the DSM. In addition to occlusion, the solar model takes into account site orientation, atmospheric effects, and variations in the sun’s position, making it a reliable tool in estimating global solar irradiation.

After the utilizable rooftop surfaces are extracted, the energy potential of rooftops is determined. The total solar electricity yield of a rooftop is calculated according to Equation 1. S_i and T_i are the total solar irradiance (in kWh/m²) and the tilt angle of the i -th utilizable segment, e and p are the efficiency and performance ratio of the photovoltaics, d is the area of each pixel of the DSM (in m²), and N is the number of utilizable segments of a rooftop. E is the total solar electricity yield of a rooftop in kWh.

$$E = d \cdot e \cdot p \cdot \sum_{i=1}^N \frac{S_i}{\cos T_i} \quad (1)$$

3 DATASETS

This study makes use of two different datasets. Dayton Annotated LiDAR Earth Scan (DALES) is the first dataset (Varney et al., 2020) used to train and evaluate PointNet++ for rooftop extraction. It is a publicly available dataset, and it contains an extensive collection of LiDAR data from a wide range of environments, making it ideal for training deep networks. It comprises 40 scenes that were manually labeled. The second dataset is part of Uppsala city in Sweden, and its LiDAR point cloud was produced by Uppsala municipality¹. It is used for plane segmentation and solar energy estimation. We manually labeled planar segments of rooftops to produce ground truth data for plane segmentation evaluation. Figure 2 shows some scenes from the datasets.

4 EXPERIMENTAL SETUP, RESULTS, AND DISCUSSION

In this section, the methodology is applied to the datasets, and the results are presented and discussed. As mentioned in Section 2.1, the first step of the methodology is to extract rooftops, which is done by utilizing PointNet++. 29 scenes out of 40 scenes from the DALES dataset are used for training, and the remaining ones are used for testing. To efficiently take advantage of the dataset, each scene is divided into

¹www.uppsala.se

small, non-overlapping tiles with a size of 50-by-50 meters. Each tile is then downsampled to contain only 9000 points, speeding up the training process. To train the deep network, the Adam optimizer with a gradient decay rate of 0.9 is used (Kingma and Ba, 2015). The maximum number of training epochs is set to 20, with each epoch consisting of 485 iterations. At the beginning of the training, the learning rate is set to 0.0005 and is reduced by a factor of 0.1 in epoch 10. Regularization is used to minimize overfitting, and the regularization factor is set to 0.1 (Murphy, 2012). The output of PointNet++ is a per-point prediction, showing which points are part of rooftops.

By applying the trained deep network to the test scenes and comparing its results (predicted rooftops) with the ground truth labels, the performance of the trained deep network for rooftop extraction is evaluated. We use accuracy and intersection over union (IOU) as two metrics to quantitatively measure the degree to which the predicted and actual labels are similar. These metrics are calculated according to Equations 2 and 3, where TP , FP , and FN are the numbers of true positives, false positives, and false negatives, respectively.

$$Accuracy = \frac{TP}{TP + FN} \quad (2)$$

$$IOU = \frac{TP}{TP + FP + FN} \quad (3)$$

Table 1 shows the evaluation results of rooftop extraction in the test scenes of the DALES dataset. We observe that the trained deep network has an accuracy of 92.60% and an IOU of 87.38% on average, showing its satisfactory performance in rooftop extraction. Thus, the trained deep network can be applied to any area. We employ it in the extraction of rooftops from the second dataset. Figure 3 shows some examples of rooftop extraction from the second dataset. The boundaries of rooftops have been extracted and regularized using α -shape (Akkiraju et al., 1995) and polyline compression (Gribov, 2019) algorithms, respectively. The figure illustrates that rooftops have been successfully separated from other objects. However, there are some cases where the trained deep network fails to correctly identify rooftops. Figure 4 shows an example where the main part of a rooftop has been missed.

Table 1: Rooftop extraction evaluation results.

	Accuracy (%)	IOU (%)
Average	92.98	87.75

In the next step, planar patches of rooftops are segmented using clustering, followed by region growing.

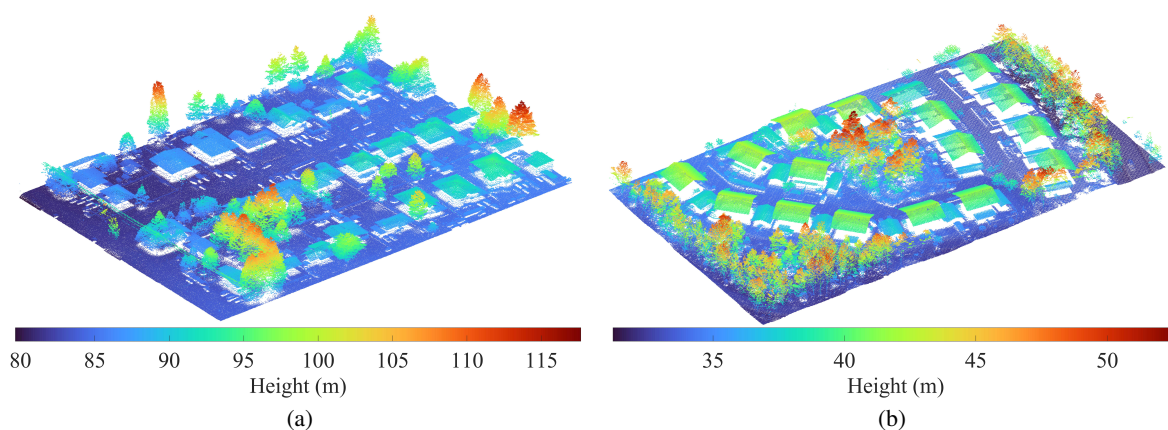


Figure 2: Sample scenes from dataset 1 (a) and dataset 2 (b).

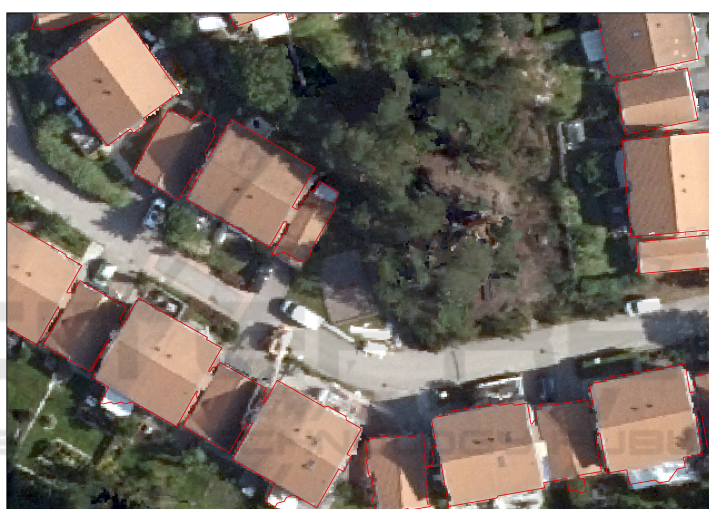


Figure 3: Some detected rooftops. The background orthophoto is only for visualization purposes.



Figure 4: Partially detected rooftop.

The MDDC algorithm used for clustering normal vectors is adaptive, that is, it does not require any input parameters. The height and angle thresholds used in region growing were set to 10 cm and 7° , obtained using trial and error in a small part of the dataset. Figure 5 shows plane segmentation results of some

rooftops. As seen in the figure, the plane segmentation method has been successful in the identification of roof faces. Minor superstructures, including vents and small chimneys, that cannot be recognized as independent planar segments appear as holes in the segments. In this way, the impact of superstructures can be considered in the identification of utilizable areas. We quantify the performance of plane segmentation by comparing its results with the ground truth data. Table 2 shows the performance of plane segmentation in terms of accuracy and IOU. It suggests that most planar segments have been accurately identified and that the method is effective.

Table 2: Plane segmentation evaluation results.

	Accuracy (%)	IOU (%)
Average	98.69	98.22



Figure 5: Plane segmentation results of some rooftops.



Solar Irradiation (kWh/m²/year)

1161

0

Figure 6: Annual global solar irradiation of some rooftops in the study area.

To pinpoint areas utilizable for photovoltaics, a solar irradiation map of rooftops is necessary, in addition to planar segments. This is due to cost-effectiveness considerations, which prevent photovoltaics from being installed over areas with low solar irradiation. Figure 6 illustrates the annual global solar irradiation distribution across some rooftops, computed with ArcGIS Desktop. The effects of shadows cast by nearby objects can be seen in this illustration.

Utilizable areas of rooftops are identified by eliminating service areas as well as geometrically unsuitable and low-irradiated areas. To remove service areas, an erosion operation whose structuring element

has a radius of 30 cm is used. To eliminate areas that cannot accommodate a photovoltaic panel, a series of opening operations are used. The size of the structuring elements of opening operations is set to 1.7 m × 1.0 m, which is the common size of a commercial rooftop photovoltaic panel. Moreover, the solar irradiation threshold SI used to remove low-irradiated areas is set to 1000 kWh/m²/year. Figure 7 shows the resulting utilizable areas of some rooftops in the dataset. As is evident from the figure, the impact of minor superstructures, highlighted by white circles, has been considered in the identification of the utilizable areas. Buffers with the width of service areas



Figure 7: Utilizable areas of rooftops in the sample scene. White circles show the impact of superstructures.

Table 3: Comparing rooftop regions with utilizable regions over the entire study area.

	Total area (m ²)	Total annual electricity yield (kWh)
Utilizable regions	699.83	90104.87
Entire rooftop regions	4224.43	403505.43
Ratio	16.57%	22.33%

have been excluded from planar segments. Moreover, some large planar segments have been discarded due to a lack of solar irradiation. It can be inferred that the methodology is able to consider the shape, orientation, and superstructures of rooftops as well as occlusions in the identification of the utilizable areas.

The total area (in m²) and annual electricity yield (in kWh) for the rooftops and their utilizable parts in the *entire* study area are shown in Table 3. The electricity yield has been estimated using Equation 1, where the efficiency and performance ratio of the photovoltaics were set to 0.16 and 0.75, respectively. According to this table, the utilizable regions based on spatially detailed analysis comprise a small proportion of the entire rooftops (16.6%), hence assessing the solar energy potential of buildings based on the entire rooftop areas may lead to an overestimation.

5 CONCLUSION

In this study, a three-step methodology was developed to estimate the solar energy potential of rooftops. Rooftops were recognized in LiDAR point clouds using deep learning. MDDC and Euclidean clustering were employed to delineate the initial planar segments of rooftops. Afterward, utilizable areas were identified by excluding geometrically unsuitable and

low-irradiated regions as well as service areas from the identified planar segments. Solar electricity yield of utilizable areas was finally estimated.

Rooftop extraction and plane segmentation were validated using ground truth data. The validation results showed that rooftops and their planar segments were successfully extracted with 93% accuracy and 88% IOU and 99% accuracy and 98% IOU, respectively. It was observed that the shape, orientation, and superstructures of rooftops and shadow effects were satisfactorily considered in the identification of utilizable areas, and thus the methodology can provide a viable means for practically valid rooftop solar energy potential estimation. The methodology is beneficial for facilitating investment decisions on photovoltaics deployment, particularly in areas where 3D city models are unavailable.

ACKNOWLEDGEMENTS

This work was partly funded by the European Regional Development Fund (ERDF), contract ID 20201871. The authors would like to thank Uppsala municipality for providing the data for this study.

REFERENCES

- Akkiraju, N., Edelsbrunner, H., Facello, M., Fu, P., Mücke, P., E., and Varela, C. (1995). Alpha Shapes: Definition and Software. In *Proceedings on International Computational Geometry Software Workshop*, Minneapolis.
- Aslani, M. and Seipel, S. (2020). A fast instance selection method for support vector machines in building extraction. *Applied Soft Computing*, 97:106716.
- Aslani, M. and Seipel, S. (2021). Efficient and decision boundary aware instance selection for support vector machines. *Information Sciences*, 577:579–598.
- Aslani, M. and Seipel, S. (2022). Automatic identification of utilizable rooftop areas in digital surface models for photovoltaics potential assessment. *Applied Energy*, 306, Part A:118033.
- Awrangjeb, M. and Fraser, C. S. (2014). Automatic Segmentation of Raw LIDAR Data for Extraction of Building Roof. *Remote Sensing*, 6(5):3716–3751.
- Bódis, K., Kougias, I., Jäger-Waldau, A., Taylor, N., and Szabó, S. (2019). A high-resolution geospatial assessment of the rooftop solar photovoltaic potential in the European Union. *Renewable and Sustainable Energy Reviews*, 114:109309.
- Byrne, J., Taminiu, J., Kurdgelashvili, L., and Kim, K. N. (2015). A review of the solar city concept and methods to assess rooftop solar electric potential, with an illustrative application to the city of Seoul. *Renewable and Sustainable Energy Reviews*, 41:830–844.
- Chen, D., Zhang, L., Mathiopoulos, P. T., and Huang, X. (2014). A Methodology for Automated Segmentation and Reconstruction of Urban 3-D Buildings from ALS Point Clouds. *IEEE Journal of Selected Topics in Applied Earth Observations and Remote Sensing*, 7(10):4199–4217.
- Fu, P. and Rich, P. M. (2000). The Solar Analyst 1.0 Manual. Technical report, Helios Environmental Modeling Institute (HEMI), USA.
- Gassar, A. A. A. and Cha, S. H. (2021). Review of geographic information systems-based rooftop solar photovoltaic potential estimation approaches at urban scales. *Applied Energy*, 291:116817.
- Gribov, A. (2019). Optimal Compression of a Polyline While Aligning to Preferred Directions. In *2019 International Conference on Document Analysis and Recognition Workshops (ICDARW)*, volume 1, pages 98–102.
- Huang, Y., Chen, Z., Wu, B., Chen, L., Mao, W., Zhao, F., Wu, J., Wu, J., and Yu, B. (2015). Estimating Roof Solar Energy Potential in the Downtown Area Using a GPU-Accelerated Solar Radiation Model and Airborne LiDAR Data. *Remote Sensing*, 7(12):17212–17233.
- Joshi, S., Mittal, S., Holloway, P., Shukla, P. R., Ó Galachóir, B., and Glynn, J. (2021). High resolution global spatiotemporal assessment of rooftop solar photovoltaics potential for renewable electricity generation. *Nature Communications*, 12(1):5738.
- Kingma, D. P. and Ba, J. (2015). Adam: A Method for Stochastic Optimization. In *International Conference on Learning Representations (ICLR)*, San Diego. Ithaca.
- Lingfors, D., Bright, J. M., Engerer, N. A., Ahlberg, J., Killinger, S., and Widén, J. (2017). Comparing the capability of low- and high-resolution LiDAR data with application to solar resource assessment, roof type classification and shading analysis. *Applied Energy*, 205:1216–1230.
- Mohajeri, N., Assouline, D., Guiboud, B., Bill, A., Gudmundsson, A., and Scartezzini, J.-L. (2018). A city-scale roof shape classification using machine learning for solar energy applications. *Renewable Energy*, 121:81–93.
- Murphy, K. P. (2012). *Machine Learning: A Probabilistic Perspective*. MIT Press, Cambridge, Massachusetts.
- Qi, C. R., Yi, L., Su, H., and Guibas, L. J. (2017). PointNet++: Deep Hierarchical Feature Learning on Point Sets in a Metric Space. In *31st Conference on Neural Information Processing Systems (NIPS 2017)*, California.
- Rich, P., Dubayah, R., Hetrick, W., and Saving, S. (1994). Using Viewshed models to calculate intercepted solar radiation: applications in ecology. *American Society for Photogrammetry and Remote Sensing Technical Papers*, pages 524–529.
- Rusu, R. B. (2009). *Semantic 3D Object Maps for Everyday Manipulation in Human Living Environments*. PhD thesis, Technical University of Munich, Munich, Germany.
- Samath, A. and Shan, J. (2010). Segmentation and Reconstruction of Polyhedral Building Roofs From Aerial LiDAR Point Clouds. *IEEE Transactions on Geoscience and Remote Sensing*, 48(3):1554–1567.
- Shin, Y.-H., Son, K.-W., and Lee, D.-C. (2022). Semantic Segmentation and Building Extraction from Airborne LiDAR Data with Multiple Return Using PointNet++. *Applied Sciences*, 12(4).
- Sundararajan, D. (2017). *Digital Image Processing A Signal Processing and Algorithmic Approach*. Springer, Singapore.
- Tasoulis, N. G. P., Hofmeyr, D. P., and K., S. (2016). Minimum Density Hyperplanes. *Journal of Machine Learning Research*, 17(156):1–33.
- Thebault, M., Clivillé, V., Berrah, L., and Desthieux, G. (2020). Multicriteria roof sorting for the integration of photovoltaic systems in urban environments. *Sustainable Cities and Society*, 60:102259.
- Varney, N., Asari, V. K., and Graehling, Q. (2020). DALES: A Large-scale Aerial LiDAR Data Set for Semantic Segmentation. In *2020 IEEE/CVF Conference on Computer Vision and Pattern Recognition Workshops (CVPRW)*, pages 717–726.